

Dihydrofolate reductase (DHFR) inhibition and molecular modeling study of some 6-bromo- or 6,8-dibromo-quinazolin-4(3H)-ones

Abdelfattah A. Abdelkhalek¹, Heba A. Ewida², Shahenda M. El-Messery³, Hossam S. A. Mahmoud¹, Ashraf F. Wasfy⁴, Esraa A. M. Moharram⁵, Hussein I. El-Subbagh⁵

¹Faculty of Oral & Dental medicine, Future University in Egypt, Cairo, Egypt

²Department of Pharmacology and Biochemistry, Faculty of Pharmaceutical Sciences & Pharmaceutical Industries, Future University in Egypt, Cairo, Egypt

³Department of Pharmaceutical Organic Chemistry, Faculty of Pharmacy, Mansoura University, Mansoura, Egypt

⁴Department of Chemistry, Faculty of Science, Benha University, Banha, Egypt

⁵Department of Medicinal Chemistry, Faculty of Pharmacy, Mansoura University, Mansoura, Egypt

ABSTRACT

Objectives: The dihydrofolate reductase (DHFR) inhibitory activity of 6-bromo- and 6,8-dibromo-quinazolin-4(3H)-ones (7–25) were studied to define the structural features and requirements that *enhance* selectivity and specificity for the proper binding to the enzyme active site.

Methods: Compounds 7–25 were tested for their *in vitro* DHFR inhibition. As an application of the use of DHFR inhibitors, *in vitro* antitumor activity using disease-oriented human cell lines assay was performed.

Key findings: Compounds 19, 20, and 22 showed remarkable DHFR inhibitory activity, inhibitory concentration (IC₅₀ 0.6, 0.2, and 0.1 μM, respectively). Compounds 12, 17, 18, 20, and 24 proved to be broad spectrum antitumor with median IC₅₀ values of 0.6, 0.6, 0.5, 0.6, and 0.7 μM, respectively. Molecular docking study results revealed that the active DHFR inhibitors 22 and 20 bind to DHFR with similar amino acid residues as methotrexate, especially Arg 28.

Conclusions: The mono-bromo series proved to be more active than the di-bromo counterparts and the 3-(2-hydrazinyl-acetyl)- is more active than its 3-(acetohydrazide) isoster. The investigated compounds could be used as template model for further optimization.

ARTICLE HISTORY

Received March 24, 2018

Accepted April 19, 2018

Published April 19, 2018

KEYWORDS

Quinazolines; DHFR inhibition; antitumor screening; molecular modeling study

Introduction

Quinazolines are among the important heterocyclic compounds which gained considerable medical attention due to their diverse scope of biological activity in the area of anticancer, antibacterial, antifungal, and antimycobacterial chemotherapy [1–5]. Dihydrofolate reductase (DHFR) is a key enzyme in folate metabolism and the biosynthesis of nucleic acids. DHFR is an important target to combat cancers and pathogenic microbes [6–11]. Several quinazoline analogs including trimetrexate (1) have been proven to exhibit DHFR inhibitory activity (Fig. 1) [9].

Several series of substituted-quinazolin-4-ones were designed and evaluated for their *in vitro* DHFR inhibition in our laboratory [12–16]. Compounds 2–6 (Fig. 1) were the most active members obtained with IC₅₀ values ranged from 0.01 to 0.4 μM. The type of substituent at positions 2-, 3-, and 6- of the quinazolin-4-ones manipulated the activity. Those previous studies revealed that recognition with the key amino acids Glu30, Ser59, Phe31, Phe34, Arg38, and Lys31 together or individually is essential for binding to DHFR receptor sites and hence, produce the needed biological activity.

Contact Hussein I. El-Subbagh ✉ subbagh@yahoo.com 📧 Department of Medicinal Chemistry, Faculty of Pharmacy, Mansoura University, Mansoura, Egypt

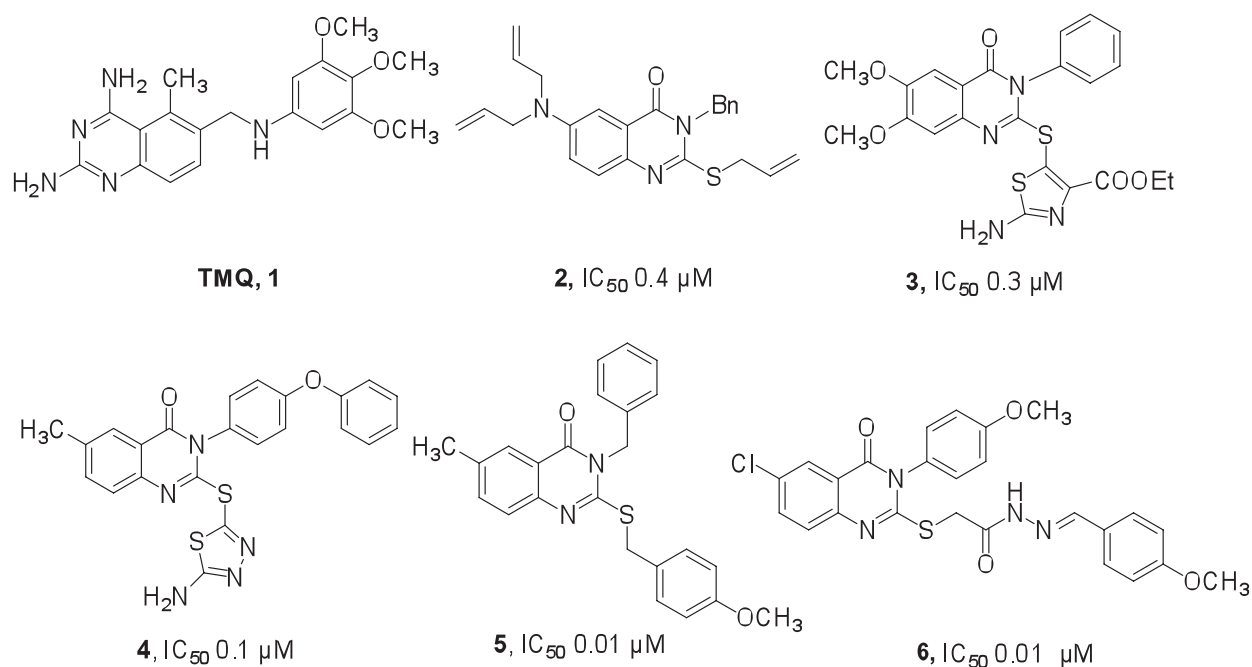


Figure 1. Structures of some lead quinazoline DHFR inhibitors.

In view of the aforementioned considerations, and in continuation to our previous efforts [12–16], the mentioned previous molecular modeling findings were used as a guide to allocate some literature of quinazoline analogs as good candidates for DHFR inhibition activity evaluation. This literature search allowed the selection of compounds 7–25 (Fig. 2), [17–19] which were resynthesized. The present study reports the DHFR inhibition activity of a series of 6-bromo- and 6,8-dibromo-quinazolin-4(3H)-one analogs accommodating 3-acetohydrazide, its isosteric analog 3-(2-hydrazinyl-acetyl)- and 4-hydrazine functions. In addition to some other analogs where the mentioned functions were utilized to introduce the benzylidene-acetohydrazide, acetyl-benzohydrazide, and its 2-oxoethyl- isosteric counterpart, 1,3,4-oxadiazole, and 1H-pyrazol-one functions. DHFR inhibition study of those quinazolines aimed to further characterize the requirements and features that enhance selectivity and specificity for the proper binding to the active site. As an application of the use of DHFR inhibitors, *in vitro* antitumor activity was also performed [20–23].

Materials and Methods

DHFR inhibition activity experiments were performed at Pharmacology Department, Faculty of Pharmacy; Future University in Egypt. Bovine liver

DHFR enzyme, methotrexate (MTX) was used in the assay (Sigma Chemical Co, USA). *In vitro* antitumor testing was conducted at The Regional Center for Mycology & Biotechnology, Al-Azhar University, Cairo, Egypt. Concerning the molecular modeling study, all experiments were conducted with Molecular Operating Environment (MOE) software. Electrostatic potential and total density maps were demonstrated using HyperChem 8.05 package from Hypercube running on a PC [24]. Enzyme structure, starting coordinate of human dihydrofolate reductase (hDHFR) enzyme in tertiary complex with reduced nicotinamide adenine dinucleotide phosphate (NADPH) and MTX, code ID 1 DLS, was obtained from the Protein Data Bank of Brookhaven National Laboratory [25]. Compounds 7–25 were previously reported [17–19].

Dihydrofolate reductase inhibition assay

The assay mixture of 50 μ M Tris-HCl buffer (pH 7.4), 50 μ M NADPH, and 10 μ l dimethyl sulfoxide (DMSO) was adjusted to a final concentration of 10^{-11} to 10^{-5} M, and 10 μ l of bovine liver DHFR, in a final volume of 1.0 ml [26–28]. After addition of the enzyme, the mixture was incubated at room temperature for 2.0 minute, and the reaction was initiated by adding 5 μ l of dihydrofolic acid, the change in absorbance ($\Delta OD/\text{minute}$) was measured by the spectrophotometer at 340 nm and 22°C, kinetic

DHFR inhibitors

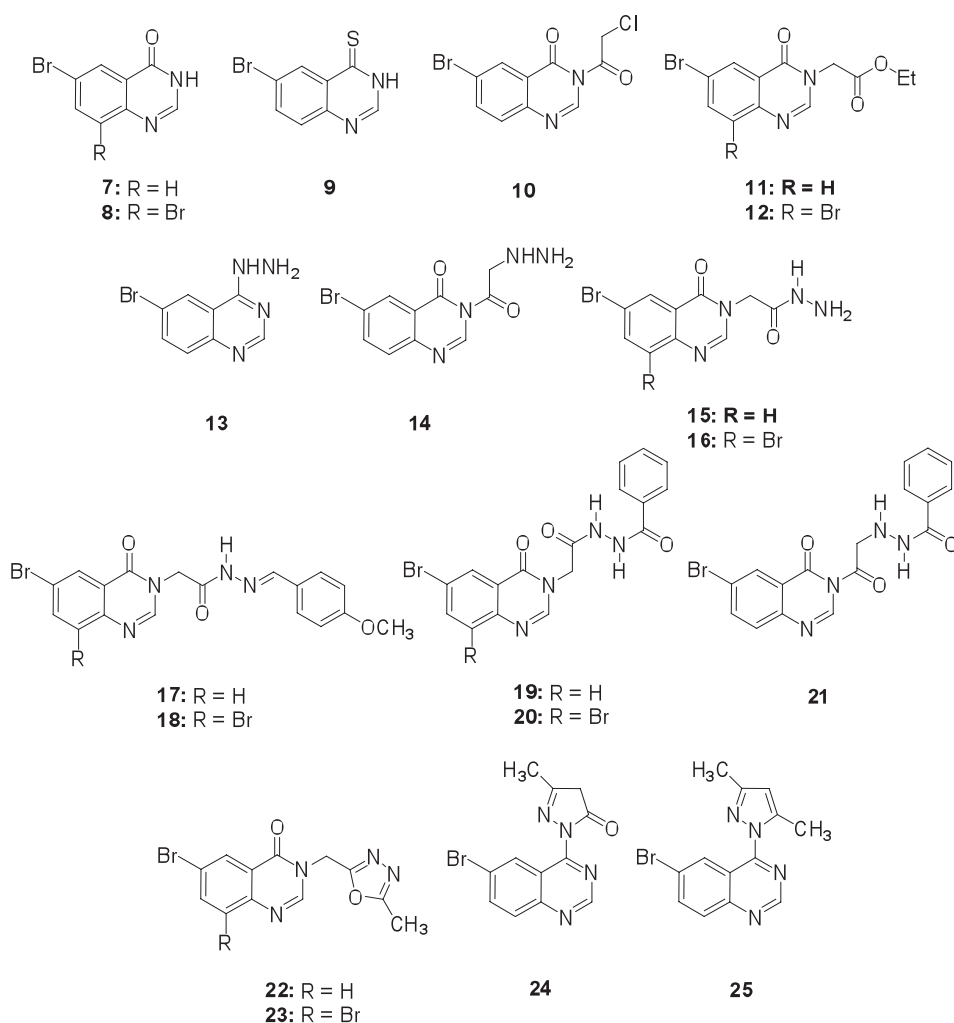


Figure 2. List of structures of the investigated compounds 7–25.

program (reading every 15 seconds for 2.5 minutes). Results were reported as % inhibition of enzymatic activity (Table 1) calculated using the following formula:

$$\text{Fractional activity of enzyme} = \frac{(\text{Sample } \Delta\text{OD/minute} - \text{blank } \Delta\text{OD/minute}) \times d}{12.3 \times V \times \text{mgP/ml}}$$

where $\Delta\text{OD/minute}$: the spectrophotometer readings

12.3: extinction coefficient for the DHFR reaction at 340 nm.

V: Enzyme volume in ml (the volume of enzyme used in the assay)

d: The dilution factor of the enzyme sample.

mgP/ml: enzyme concentration of the original sample before dilution.

In vitro antitumor screening

Cell lines were grown under a sterile condition, in RPMI 1640 media (Gibco, NY) supplemented with

10% fetal bovine serum (Biocell, CA), 5×10^5 cell/ml was used to test the growth inhibition activity of the synthesized compounds. The concentrations of the compounds ranging from 0.01 to 100 μM were prepared in phosphate buffer saline. Each compound was initially solubilized in DMSO, however, each final dilution contained less than 1% DMSO. Solutions of different concentrations (0.2 ml) were pipetted into separate well of a microtiter tray in duplicate. Cell culture (1.8 ml) containing a cell population of 6×10^4 cells/ml was pipetted into each well. Controls, containing only phosphate buffer saline and DMSO at identical dilutions, were also prepared in the same manner. These cultures were incubated in a humidified incubator at 37°C. The incubator was supplied with 5% CO_2 atmosphere. After 48 hours, cells in each well were diluted 10 times with saline and counted by using a Coulter counter. The counts were corrected for the dilution [19–22,29], (Table 1).

Table 1. DHFR inhibition activity (IC_{50} , μM) and antitumor screening (GI%, IC_{50} , μM) of compounds 7–25 against the human cancer lines Skin A-431, Lung A-549, Colon HCT-116, and hepatocellular Hep-G2 carcinomas.

Compound	DHFR inhibition (IC_{50} , μM)	GI% (IC_{50} , μM)				Median GI% (IC_{50} , μM)
		A-431	A-549	HCT-116	Hep-G2	
7	4.7 ± 0.2	2.0	1.8	0.5	0.4	1.2
8	15.9 ± 0.1	1.5	1.6	0.5	0.6	1.1
9	11.9 ± 1	4.3	2.4	1.2	1.3	2.3
10	48.2 ± 1	2.8	1.1	0.4	0.5	1.2
11	5.9 ± 0.4	1.8	0.7	0.6	0.6	0.9
12	6.5 ± 0.7	1.5	0.6	0.2	0.2	0.6
13	35.9 ± 0.1	4.3	2.9	4.0	2.6	3.5
14	12.7 ± 0.8	1.1	0.8	0.8	0.6	0.8
15	48.2 ± 1	1.9	1.2	1.0	1.1	1.3
16	4.4 ± 0.5	1.8	1.0	1.5	0.9	1.3
17	21.4 ± 0.7	1.4	0.5	0.2	0.2	0.6
18	14.6 ± 1.0	1.1	0.4	0.3	0.2	0.5
19	0.6 ± 0.003	1.2	1.2	0.3	0.7	0.9
20	0.2 ± 0.003	1.0	0.8	0.1	0.5	0.6
21	1.9 ± 0.01	1.8	1.0	1.1	0.3	1.1
22	0.1 ± 0.01	1.2	1.0	0.2	0.7	0.8
23	2.5 ± 0.03	3.1	1.5	0.6	0.5	1.4
24	>100	2.0	0.3	0.2	0.2	0.7
25	67.9 ± 1.9	1.2	0.7	0.4	0.9	0.8
MTX	0.08	1.0	0.8	0.5	0.5	0.7

Docking and molecular modeling study

The three-dimensional structures of the substituted quinazoline derivatives, which presented best and worst biological profiles, in their neutral forms, were constructed using the MOE of Chemical Computing Group Inc software [24]. Lowest energy conformer of each new analog “global minima” was docked into the hDHFR enzyme-binding domain. Starting coordinate of hDHFR enzyme in tertiary complex with reduced NADPH and MTX, code ID 1 DLS, was obtained from the Protein Data Bank of Brookhaven National Laboratory [25]. All of the hydrogens were added and enzyme structure was subjected to refinement protocol in which the constraints on the enzyme were gradually removed and minimized until the rms gradient was 0.01 kcal/mol Å. The energy minimization was carried out using the molecular mechanics force field “AMBER.” The energy-minimized structure was used for molecular modeling studies keeping all the heavy atoms fixed until an RMSD gradient of 0.05 kcal/mol Å was reached. Ligand structures were built with MOE and minimized using the MMFF94x forcefield until an RMSD gradient of 0.05 kcal/mol Å was reached. For each analog, energy minimizations were performed using 1,000 steps of steepest descent followed

by conjugate gradient minimization to an RMSD energy gradient of 0.01 kcal/mol Å. The active site of the enzyme was defined using a radius of 10.0 Å around MTX. Energy of binding was calculated as the difference between the energy of the complex and individual energies of the enzyme and ligand [13,30–34]. The docking was performed using the Alpha Triangle placement method and the London dG scoring method. Three hundred results for each ligand were generated, discarding the results with an RMSD value >3 Å. The best scored result of the remaining conformations for each ligand was further analyzed. The protein/ligand complexes were minimized using the MMFF94x force field, until an RMSD gradient of 0.1 kcal/mol Å was reached.

Flexible alignment and superposition

The investigated compounds were subjected to flexible alignment and superposition experiments using “MOE” software (MOE of Chemical Computing Group Inc., on a Core 2 duo 2.3 GHz workstation). The molecules were built using the Builder module of MOE. Their geometry was optimized by using the MMFF94 forcefield followed by a flexible alignment using systematic conformational search. Lowest energy aligned conformation(s) were identified [35].

Electrostatic potential isosurface maps

Molecular structure of the selected compounds was constructed from fragment libraries in the HyperChem program [34]. The partial atomic charges for each analog were assigned with the semiempirical mechanical calculation method "AM1" implemented in HyperChem 8.05. Conformational search was formed around all the rotatable bonds with an increment of 10° using conformational search module as implemented in HyperChem 6.03. All the conformers were minimized until the rms deviation was $0.01 \text{ kcal/mol \AA}$.

Results and Discussion

In vitro dihydrofolate reductase inhibition

The investigated compounds 7–25 were evaluated as inhibitors of bovine liver DHFR which possess 75% resemblance to human DHFR, using reported procedures [26–28]. Results were shown as IC_{50} values (μM) in Table 1. Compounds 19, 20, and 22 expressed remarkable DHFR inhibitory potency, (IC_{50} 0.6, 0.2, and $0.1 \mu\text{M}$, respectively), in comparison to MTX (IC_{50} , 0.08 mM) which was used as a positive control. Compounds 7, 11, 12, 16, 21, and 23 showed moderate DHFR inhibition with IC_{50} values range of 1.9 – $6.5 \mu\text{M}$; while the rest of test compounds were of weak activity.

In vitro antitumor screening

As an application of the use of DHFR inhibitors, compounds 7–25 were evaluated for their antitumor activity against the human cancer lines Skin A-431, Lung A-549, Colon HCT-116, and hepatocellular Hep-G2 carcinomas. The National Cancer Institute *in vitro* protocol was adopted using MTX as positive control [19–22,29]. The results were reported as IC_{50} (μM) of the test compounds causing tumor growth inhibition (Table 1). All of the tested compounds exhibited antitumor potency of various magnitudes. Compounds 12, 17, 18, 20, and 24 showed remarkable broad spectrum antitumor potency and considered to be the most active members in this study with median IC_{50} values of 0.6 , 0.6 , 0.5 , 0.6 , and $0.7 \mu\text{M}$, respectively. Some compounds showed selectivity toward the used tumor cell lines, such as 8, 19, and 22 against Colon HCT-116 (0.5 , 0.3 , and $0.2 \mu\text{M}$, respectively), 11 and 14 against Lung A-549 (0.7 and $0.8 \mu\text{M}$, respectively). In this study, the antitumor properties of compounds 19, 20, and 22 are most likely due to their potent inhibition of the enzyme DHFR; while compounds 10, 17,

24, and 25 exert their antitumor potency with some other mode of action.

Structure–activity correlation

In the present study, two series of compounds were studied, 6-bromo- and 6,8-dibromo-quinazolin-4(3H)-ones. Structure–activity correlation study of the employed two series helped to clarify the discrepancy of biological activity among the investigated compounds. In the 6-bromo series, the introduction of 3-(2-chloroacetyl)- function to 7 ($4.7 \pm 0.2 \mu\text{M}$) produced 10 ($48.2 \pm 1 \mu\text{M}$) with marked decrease in the DHFR inhibition activity. Reacting 10 with hydrazine hydrate afforded the 3-(2-hydrazinyl-acetyl)- analog (14, $12.7 \pm 0.8 \mu\text{M}$) with a 4-fold increase in activity. Upon converting 14 into the benzohydrazide 21 ($1.9 \pm 0.01 \mu\text{M}$), a remarkable increase in the DHFR inhibition activity was noticed. Thiation of 7 ($4.7 \pm 0.2 \mu\text{M}$) produced the 4-thione derivative 9 ($11.9 \pm 1 \mu\text{M}$) with a 2-fold decrease in activity. The introduction of 3-ethyl acetate function to compound 7 ($4.7 \pm 0.2 \mu\text{M}$) produced 11 ($5.9 \pm 0.4 \mu\text{M}$) with almost the same potency. Reacting 11 with hydrazine hydrate followed by benzoyl chloride gave 19 ($0.6 \pm 0.003 \mu\text{M}$) and its cyclization afforded the 1,3,4-oxadiazol 22 ($0.1 \pm 0.01 \mu\text{M}$), the most active members of this study. Reacting 9 with hydrazine hydrate afforded 13 ($35.9 \pm 0.1 \mu\text{M}$) with dramatic decrease in activity. Compound 13 were further used to prepare 3-methyl-1H-pyrazol-5(4H)-one (24); and 3,5-dimethyl-1H-pyrazol (25) analogs with total loss of activity. The presence of the 1H-pyrazol at the 4- position of the quinazoline ring and loss of activity confirms the necessity of the presence of 4-carbonyl moiety mentioned as a pharmacophoric requirement of this class of DHFR inhibitors [10–14]. In general, the mono-bromo series proved to be more active than the di-bromo counterparts and the 3-(2-hydrazinyl-acetyl)- is more active than its 3-(acetohydrazide) isosters. The same analogy could be applied for the obtained antitumor activity results.

Molecular modeling study

In order to understand and interpret the DHFR inhibitory pattern of this class of compounds, molecular modeling study was essentially needed. A comparative modeling study of the most active DHFR inhibitors 20 and 22 and the least active 24 against MTX was initiated. The tertiary complex of hDHFR crystal structure (pdb ID: 1 DLS obtained

from the protein data bank), NADPH and MTX were used as references for modeling and docking [25]. Conformational analysis of 20, 22, and 24 has been performed. The least energy conformer for each compound was obtained by conformational searching in torsional space using the multi-conformer method and is illustrated in Figure 3. A comparative docking studies between the active DHFR inhibitors 20 and 22 and the inactive counterpart 24 against MTX was performed. The tertiary complex used showed tight binding and ionic bonding of the cation of N1/2-NH₂ group to Glu30. MTX binds to DHFR by Arg28, Arg70, Asn64, Lys68, Val115, and Ile7 amino acid residues [13,30–34]. Docking results revealed that 22 showed high affinity with a binding energy of -11.2487 kcal/mol with Arg28 via hydrogen bonding interaction (66%) and Phe31 residue through arene–arene interaction (Fig. 4a). Moreover, Compound 20 binds with good affinity (binding energy of -10.8776 kcal/mol) with Arg28 by arene–cation interaction and Ser59 through hydrogen binding interaction via its carbonyl group (Fig. 4b). On the contrary, the inactive DHFR inhibitor 24 did not interact with any amino acid residue in the active site explaining their inactivity profile despite the similarity in structure to the active candidates. A detailed view of both 22 and 20 into the active site showed that they occupy a deeper location into the cavity which causes the higher binding

interaction with the hydrophobic residues in the DHFR active site (Fig. 5a and b).

To show similarity between the 3-D structures of the most active 22 and 20, from one side and the inactive 24 from the other side, flexible alignment [35] was employed. The top scoring alignment with the least strain energy is shown in (Fig. 6a) where a good alignment between 22 and 20 was obtained. On the contrary, (Fig. 6b) clearly shows different alignment profiles between 22 and 24 which interpret their different activity pattern. In a search for reasons behind the different affinity of the investigated compounds toward DHFR binding, hydrophobic surface mapping study was performed. Compounds 22 and 20 clearly showed a preference for more hydrophobic regions (Fig. 7a and b) that could be attributed to the presence of the bromo moiety on the phenyl part of quinazoline in both compounds causing higher lipophilic character of the intact molecule. On the contrary, examination of surface mapping of the inactive 24 showed less greener areas and more red to blue regions (Fig. 7c) indicates higher hydrophilicity and hence, less binding.

Conclusion

In conclusion, compounds 7–25 represent a series of 6-bromo- and 6,8-dibromo-quinazolin-4(3H)-ones. Compounds 19, 20, and 22 showed remarkable DHFR inhibitory potency, (IC₅₀ 0.6, 0.2, and 0.1 μ M,

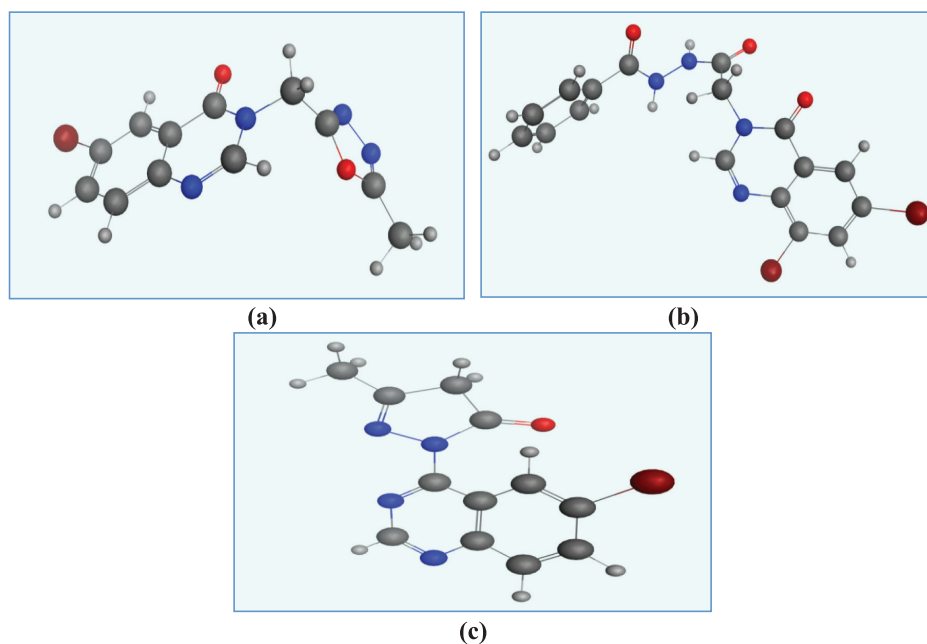


Figure 3. Lowest energy conformers of the active 22 (a), 20 (b); and the inactive 24 (c) with balls and cylinders.

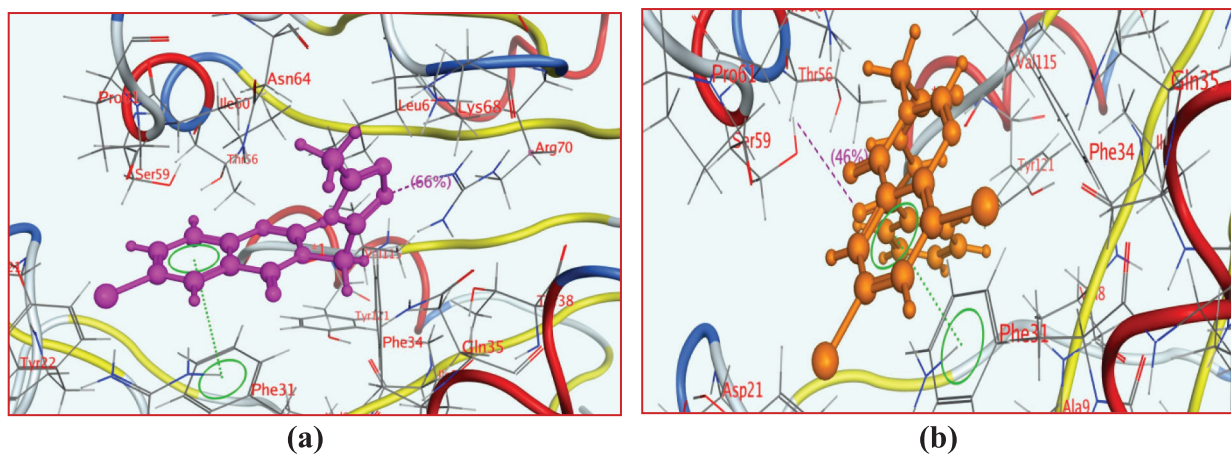


Figure 4. 3-D Binding mode and residues involved in the recognition of: (a) 22 (IC_{50} $0.1 \pm 0.01 \mu\text{M}$) and (b) 20 (IC_{50} $0.2 \pm 0.003 \mu\text{M}$) docked and minimized in the DHFR binding pocket.

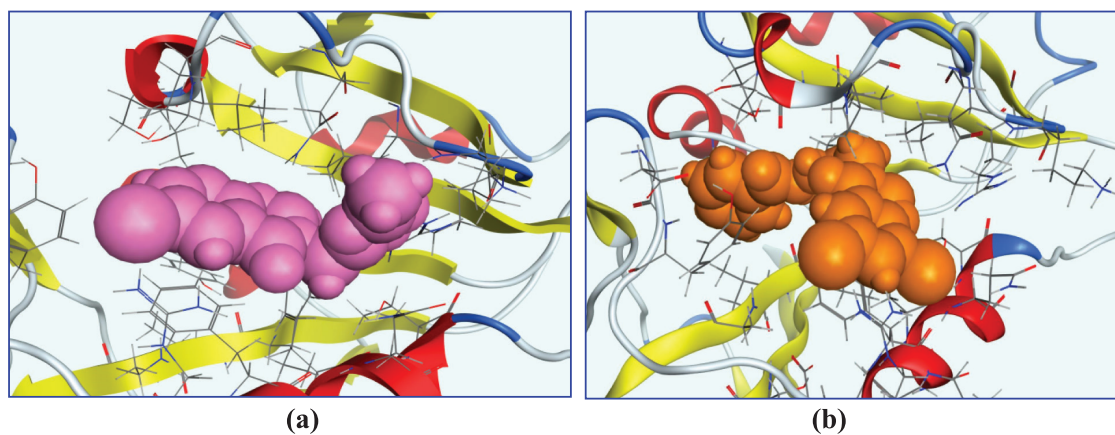


Figure 5. The aligned conformation of the most active 22, pink (a) and 20, orange (b) occupying the DHFR binding pocket.

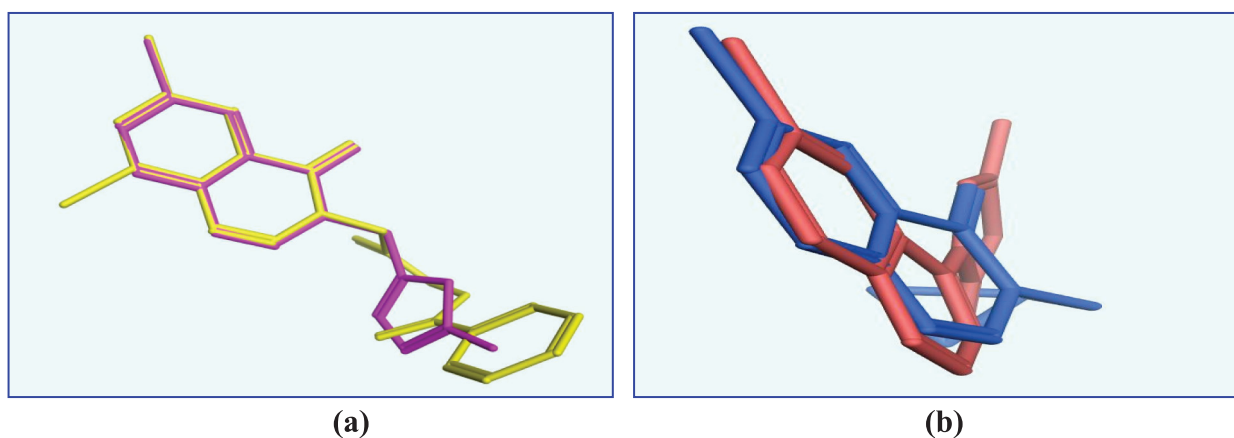


Figure 6. (a) Flexible alignment of the active compounds 22 (pink) and 20 (yellow); (b) Flexible alignment of the active 22 (pink) and the inactive 24 (blue)..

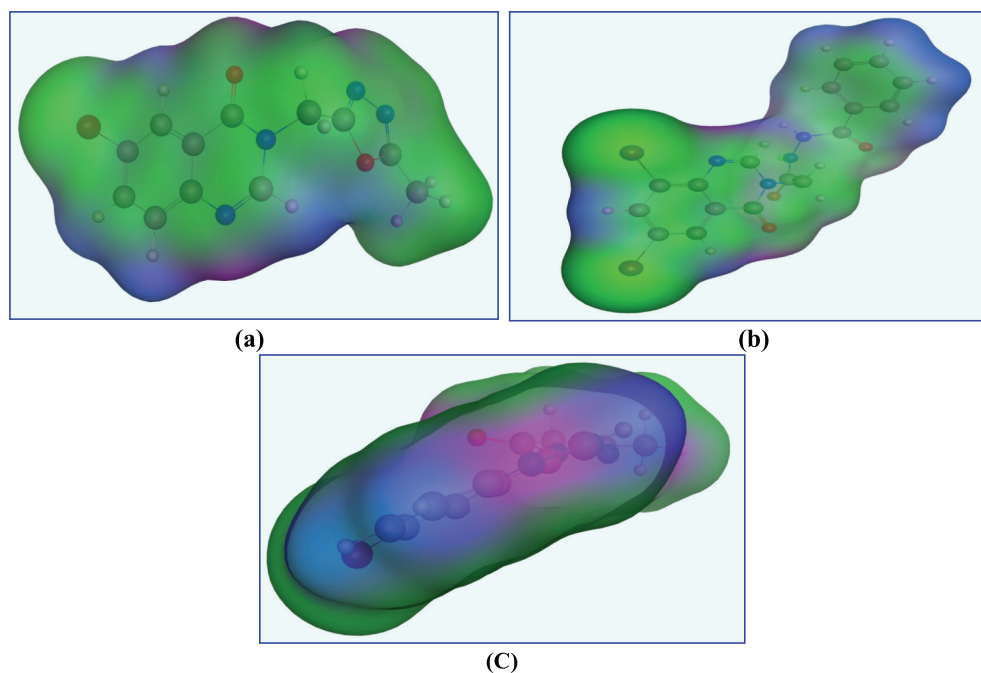


Figure 7. Surface map for compounds (a) 22, (b) 20, and (c) 24 in pocket site (Pink: hydrogen bond, blue: mild polar, and green: hydrophobic).

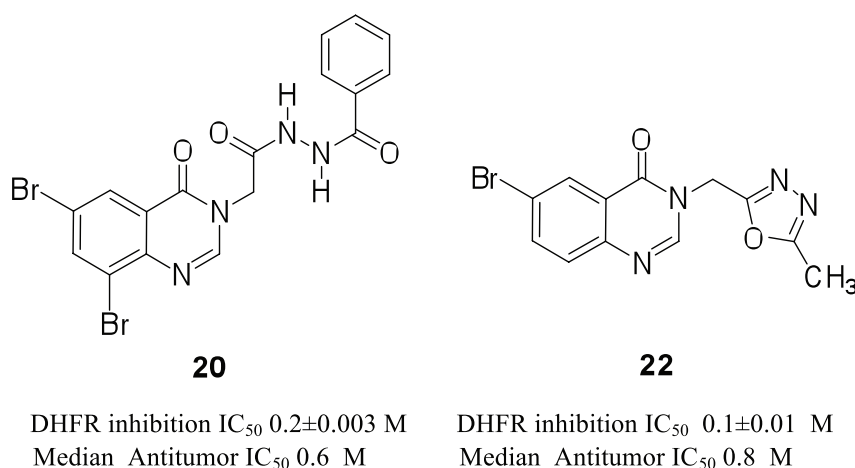


Figure 8. Structures of the most active compounds 20 and 22.

respectively), in comparison to MTX (IC_{50} , $0.08 \mu\text{M}$). Compounds 12, 17, 18, 20, and 24 showed remarkable broad spectrum antitumor potency and considered to be the most active members in this study with median IC_{50} values of 0.6, 0.6, 0.5, 0.6, and $0.7 \mu\text{M}$, respectively. In general, the mono-bromo series proved to be more active than the di-bromo counterparts and the 3-(2-hydrazinyl-acetyl)- is more active than its 3-(acetohydrazide) isomers in the involved biological activities. Molecular docking study results revealed that active DHFR inhibitor candidates 22 and 20 (Fig. 8) bind to DHFR with similar amino acid residues as MTX, especially Arg28, which support the hypothesis that these compounds could exert

their antitumor action via DHFR inhibition. The investigated compounds could be used as template models for further optimization.

REFERENCES

- [1] Connolly DJ, Cusack D, Sullivan TPO, Guiry PJ. Synthesis of quinazolinones and quinazolines. *Tetrahedron* 2005; 61:10153–202.
- [2] Mhaske SB, Argade NP. The chemistry of recently isolated naturally occurring quinazolinone alkaloids. *Tetrahedron* 2006; 62:9787–826.
- [3] Mahato AK, Srivastava B, Nithya S. Chemistry, structure activity relationship and biological activity of quinazolinone-4(3H)-one derivatives. *Med Chem* 2011; 2:1–6.

- [4] Patel NB, Patel JC. Synthesis and antimicrobial activity of Schiff bases and 2-azetidinones derived from quinazolin-4(3H)-one. *Arabian J Chem* 2011; 4:403–11.
- [5] Cakici M, Catir M, Karabuga S, Kilic H, Ulukanli S, Gulluce M, et al. Synthesis and biological evaluation of (*S*)-4-aminoquinazoline alcohols. *Tetrahedron Asymm* 2010; 21:2027–31.
- [6] Masur H. Problems in the management of opportunistic infections in patients with human immunodeficiency virus. *J Infect Dis* 1990; 161:858–64.
- [7] Berman EM, Werbel LM. The renewed potential for folate antagonists in contemporary cancer chemotherapy. *J Med Chem* 1991; 34:479–85.
- [8] Gonen N, Assaraf YG. Antifolates in cancer therapy: structure, activity and mechanisms of drug resistance. *Drug Resist Updates* 2012; 15:183–210.
- [9] Elslager EF, Johnson JL, Werbel LM. Folate antagonists. 20. Synthesis and antitumor and antimalarial properties of trimetrexate and related 6-[(phenylamino)methyl]-2,4-quinazolinediamines. *J Med Chem* 1983; 26:1753–60.
- [10] Tonelli M, Naesens L, Gazzarrini S, Santucci M, Cichero E, Tasso B, et al. Host dihydrofolate reductase (DHFR)-directed cycloguanil analogues endowed with activity against influenza virus and respiratory syncytial virus. *Eur J Med Chem* 2017; 135:467–78.
- [11] Sharma M, Chauhan PM. Dihydrofolate reductase as a therapeutic target for infectious diseases: opportunities and challenges. *Future Med Chem* 2012; 4:1335–65.
- [12] Al-Omary FAM, Abou-zeid LA, Nagi MN, Habib EE, Abdel-Aziz AA-M, El-Azab AS, et al. Non-classical antifolates. Part 2: synthesis, biological evaluation, and molecular modeling study of some new 2,6-substituted-quinazolin-4-ones. *Bioorg Med Chem* 2010; 18:2849–63.
- [13] Al-Omary FAM, Hassan GS, El-Messery SM, Nagi MN, Habib EE, El-Subbagh HI. Nonclassical antifolates, part 3: synthesis, biological evaluation and molecular modeling study of some new 2-heteroarylthio-quinazolin-4-ones. *Eur J Med Chem* 2013; 63:33–45.
- [14] Al-Rashood ST, Hassan GS, El-Messery SM, Nagi MN, Habib EE, Al-Omary FAM, et al. Synthesis, biological evaluation and molecular modeling study of 2-(1,3,4-thiadiazolyl-thio and 4-methylthiazolyl-thio)-quinazolin-4-ones as a new class of DHFR inhibitors. *Bioorg Med Chem Lett* 2014; 24:4557–67.
- [15] El-Gazzar YI, Georgey HH, El-Messery SM, Ewida HA, Hassan GS, Raafat MM, et al. Synthesis, biological evaluation and molecular modeling study of new (1,2,4-triazole or 1,3,4-thiadiazole)-methylthio-derivatives of quinazolin-4(3H)-one as DHFR inhibitors. *Bioorg Chem* 2017; 72:282–92.
- [16] Ewida MA, Abou El Ella DA, Lasheen DS, Ewida HA, El-Gazzar YI, El-Subbagh HI. Thiazolo [4,5-*d*] pyridazine analogues as a new class of dihydrofolate reductase (DHFR) inhibitors: synthesis, biological evaluation and molecular modeling study. *Bioorg Chem* 2017; 74:228–37.
- [17] Mohamed MS, Kamel MM, Kassem EM, Abotaleb N, Abd El-Moez SI, Ahmed MF. Novel 6,8-dibromo-4(3H)-quinazolinone derivatives of anti-bacterial and anti-fungal activities. *Eur J Med Chem* 2010; 45:3311–9.
- [18] Mosaad MS, Mohsen KM, Emad KMM, Abotaleb N, Nofal SM, Ahmed FM. Novel 6,8-dibromo-4(3H)-quinazolinone derivatives of promising anti-inflammatory and analgesic properties. *Acta Poloniae Phar. Drug Res* 2010; 67:159–71.
- [19] Mahmoud HSA. Synthesis of heterocyclic nitrogen compounds bearing nucleoside moiety with anticipated antitumor activity. Master thesis, Department of chemistry, Faculty of Science, Benha University, Banha, Egypt, 2016.
- [20] Grever MR, Schepartz SA, Chabner BA. The National Cancer Institute: cancer drug discovery and development program. *Semin Oncol* 1992; 19:622–38.
- [21] Monks A, Scudiero D, Skehan P. Feasibility of a high-flux anticancer drug screen using a diverse panel of cultured human tumor cell lines. *J Natl Cancer Inst* 1991; 83:757–66.
- [22] Boyd MR, Paull KD. Some practical considerations and applications of the national cancer institute in vitro anticancer drug discovery screen. *Drug Rev Res* 1995; 34:91–109.
- [23] Skehan P, Storeng R, Scudiero D, Monks A, McMahon J, Vistica D, et al. New colorimetric cytotoxicity assay for anticancer-drug screening. *J Natl Cancer Inst* 1990; 82:1107–12.
- [24] Hyperchem. Molecular modeling system. Hypercube Inc, Release 6, Gainesville, FL, 1999.
- [25] Nordberg MG, Kolmodin K, Aqvist J, Queener SF, Hallberg P. Design, synthesis, and computational affinity prediction of ester soft drugs as inhibitors of dihydrofolate reductase from *Pneumocystis carinii*. *Eur J Pharm Sci* 2004; 22:43–53.
- [26] Adamson C, Balis M, McCully L, Godwin S, Poplack G. Methotrexate pharmacokinetics following administration of recombinant carboxypeptidase-G2 in rhesus monkeys. *J Clin Oncol* 1992; 10:1359–64.
- [27] Falk C, Clark R, Kalman M. Enzymatic assay for methotrexate in serum and cerebrospinal fluid. *Clin Chem* 1976; 22:785–8.
- [28] Pignatello R, Sapmpinato G, Sorrenti V, Vicari L, Di-Giacomo C, Vanella A, et al. Synthesis and preliminary in vitro screening of lipophilic alpha, gamma-bis(amides) as potential prodrugs of methotrexate. *Anticancer Drug Des* 1996; 11:253–64.
- [29] El-Subbagh HI, El-Sherbeny MA, Nasr MN, Goda FE, Badria FA. Novel diarylsulphide derivatives as

- potential cytotoxic agents. *Boll Chim Farm* 1995; 134:80–4.
- [30] Stockman BJ, Nirmala NR, Wanger G, Delcamp TJ, DeYarman MT, Freisheim JH. Methotrexate binds in a non-productive orientation to human dihydrofolate reductase in solution, based on NMR spectroscopy. *Fed Eur Biochem Soc Lett* 1991; 283:267–9.
- [31] Profeta S, Allinger NL. Molecular mechanics calculations on aliphatic amines. *J Am Chem Soc* 1985; 107:1907–18.
- [32] Allinger NL. Conformational analysis. 130. MM2. A hydrocarbon force field utilizing V1 and V2 torsional terms. *J Am Chem Soc* 1977; 99:8127–34.
- [33] Labute P, Williams C, Feher M, Sourial E, Schmidt JM. Flexible alignment of small molecules. *J Med Chem* 2001; 44:1483–90.
- [34] Kearsley S, Smith GM. An alternative method for the alignment of molecular structures: maximizing electrostatic and steric overlap. *Tetrahedron Comput Methodol* 1990; 3:615–33.
- [35] Cody V, Schwalbe CH. Structural characteristics of antifolate dihydrofolate reductase enzyme interactions. *Crystallog Rev* 2006; 12:301–33.